Near-IR Diffuse Interstellar Bands in SDSS-III APOGEE Spectra

G. Zasowski[1,2,3] **and B. Ménard**[3,4,5]

[1]NSF Postdoctoral Fellow, email: `gail.zasowski@gmail.com`

[2]Department of Astronomy, The Ohio State University,
140 West 18th Ave, Columbus, OH, 43210, USA

[3]Department of Physics & Astronomy, Johns Hopkins University,
3400 North Charles Street, Baltimore, MD 21218, USA

[4]Kavli IPMU (WPI), University of Tokyo, Kashiwa 277-8583, Japan

[5]Alfred P. Sloan Fellow

Abstract. Using high resolution H-band spectra from first-year observations of the SDSS-III APOGEE survey, we have searched for the presence of Diffuse Interstellar Bands (DIBs) towards several thousand stars and obtained $\sim$7 000 robust detections spanning a broad range of Galactic environments. This represents the largest homogeneous sample of DIB systems in terms of both size and sky coverage, which can be used for various statistical studies. For example, we find the strength of the most prominent near-IR DIB (at $1.5723\,\mu$m) to be strongly correlated with line-of-sight dust extinction, and its apparent velocity appears to trace that of the Galactic CO emission. The ability to work at near-IR wavelengths allows us to probe lines of sight penetrating through the dusty disk of the Galaxy, spanning a range of about 8 magnitudes of extinction. This preliminary investigation illustrates how a large sample of DIBs can serve as a useful tool to probe the structure of the Galaxy and the chemistry of the interstellar medium.

Keywords. Spectroscopy: absorption lines, stars, ISM

1. Introduction

Nearly a century ago, astronomers such as Heger (1922) and Merrill (1936) noticed additional absorption features superimposed on optical stellar spectra, between $5700\,\text{Å} \lesssim \lambda \lesssim 6700\,\text{Å}$. These features were broad (relative to other interstellar lines) and appeared more strongly in sources behind diffuse interstellar material than those behind, say, dense molecular clouds. As numerous other features with similar traits were identified, they were given the collective name "diffuse interstellar bands" (DIBs). Studies of DIBs often focus on a few features in dozens-to-hundreds of stars (e.g., McCall *et al.* 2002; Raimond *et al.* 2012) or on hundreds of features in a small number of stars at very high spectral resolution (e.g., Hobbs *et al.* 2008, 2009). No physical carrier has yet been positively identified as the source of these bands, but more than 500 of them have been tabulated at UV-optical wavelengths.

In contrast, no DIBs were identified at infrared (IR) wavelengths until 1990, with the detection of two in the J-band (Joblin *et al.* 1990). Geballe *et al.* (2011) published the first detections of H-band DIBs — 13 features observed in most or all of about a half-dozen stars towards the Galactic Center and the Cygnus OB2 association. Since then, additional features have been reported in both the J- and H-bands, bringing the census of near-IR DIB detections to a couple dozen distinct features measured in dozens of stars (Cox *et al.* this volume).

In this proceeding, we expand the number of measurements by nearly an order of magnitude and describe the largest sample of near-IR DIB detections to date — the strongest H-band feature (at 1.5723 μm) in the spectra of nearly 7 000 stars from the SDSS-III APOGEE survey. Unlike the early-type dwarf stars typically observed in DIB studies, our sample comprises highly luminous red giants that probe the interstellar medium (ISM) up to several kiloparsecs from the Sun. The large size of the sample, and its distribution throughout the Galactic disk, make these DIBs not only clues to the interstellar chemistry that produces the absorption features but also powerful tools with which to study Galactic-scale structure and kinematics.

2. The data

APOGEE and ASPCAP: The Apache Point Observatory Galactic Evolution Experiment (APOGEE; Majewski 2012), one of the four experiments comprising the Sloan Digital Sky Survey III (SDSS-III; Eisenstein *et al.* 2011), is a high resolution ($R \sim 22\,500$) H-band (1.51 μm $< \lambda <$ 1.70 μm) spectroscopic survey of $\sim 10^5$ 2MASS-selected red giant stars spanning the Milky Way's bulge, disk, and halo (Zasowski *et al. submitted*). With precise radial velocities (RVs), stellar parameters (e.g., $T_{\rm eff}$, $\log g$, [Fe/H], [α/Fe]) and up to 15 elemental abundances for each star, APOGEE's primary goal is studying the formation and chemodynamical evolution of the Galaxy. Our analysis draws from $\sim 60\,000$ stars observed during the survey's first year of observations, from September 2011 to July 2012.

Stellar properties and abundances are determined by the APOGEE Stellar Parameters and Chemical Abundances Pipeline (ASPCAP; Garcia Perez *et al. in prep*), which performs a multi-dimensional χ^2-minimization between the observed spectra and a large grid of synthetic stellar spectra. Comparison to standard stars and well-studied clusters indicate that the current pipeline produces parameters accurate to a few 100 K in $T_{\rm eff}$, a few 0.1 dex in $\log g$, and a few 0.1 dex in [Fe/H] (Mészáros *et al. submitted*), within specified parameter ranges.

Residual Spectra: For each star in the sample we consider the continuum normalized spectrum $R(\lambda)$, obtained by dividing the observed spectrum $F(\lambda)_{\rm obs}$ by its best-fitting synthetic spectrum. To first order, $R(\lambda)$ is expected to be consistent with unity. In practice, various features can be detected: interstellar absorption lines, inadequately corrected telluric absorption and emission in $F(\lambda)_{\rm obs}$, and poorly fitted stellar absorption lines. The latter two can be identified by their wavelength dependence. Telluric and stellar residuals appear at fixed wavelengths in the observed and stellar rest frames, respectively. In contrast, absorption features arising from the ISM unrelated to the background star vary in wavelength in both frames, since the ISM velocity is independent of the stellar RV.

We have visually examined numerous $R(\lambda)$ spectra, built a catalog of features, and then classified each of them as telluric, stellar, or interstellar in origin based on its wavelength behavior across multiple stars. We also cross-matched these residuals with known prominent telluric, stellar, and interstellar features. Only candidate absorption lines classified as interstellar (all of which are broad enough that we refer to them as DIBs hereafter) are explored in the analysis described below.

DIB Extraction: We focus here on the H-band DIB located at 1.5723 μm, first reported by Geballe *et al.* (2011). In each residual spectrum $R(\lambda)$ we search for this band by fitting a Gaussian-shaped absorption profile at the expected wavelength (within 5 Å) and estimating its observed wavelength and equivalent width, EqW. Some studies (e.g., Drosback *et al.* 2005) have explored the use of non-Gaussian profile shapes, such as
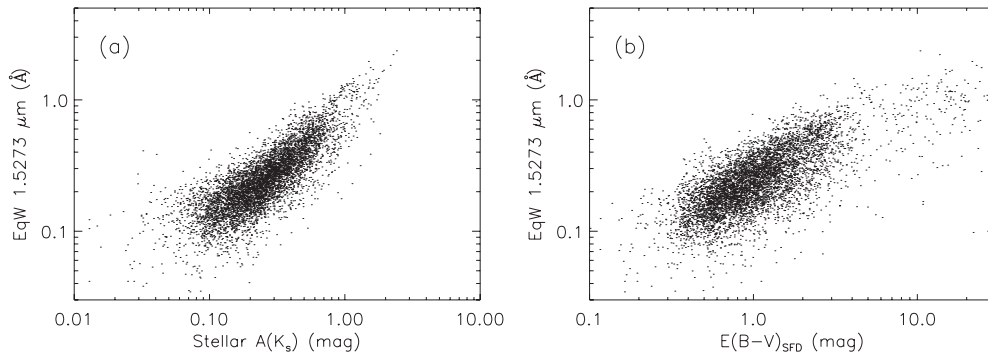
Figure 1. (a): Comparison between equivalent width of $1.5723\,\mu$m DIB and RJCE stellar extinction $A(K_s)$. (b): Comparison between equivalent width of $1.5723\,\mu$m DIB and SFD reddening $E(B-V)$.

Lorentzian or Drude functions, and others have noted the asymmetric shapes of many of the optical bands. This higher level of complexity will be added in future iterations.

Identifying robust DIBs: For this preliminary analysis we aim for purity but not completeness; we create a catalog of DIBs that includes only the most reliable absorption lines. We keep only the systems for which the spectrum S/N is at least 65 per pixel, the stellar RV determination is robust, the χ^2 of the ASPCAP fit is low, the stellar parameters are not close to the edges of the synthetic model grid, and the Gaussian fit to the absorption feature provides a detection at the 2σ significance level. The exact definitions of these criteria, expected to evolve as APOGEE's data reduction pipeline and ASPCAP continue to improve, will be presented elsewhere. Finally, we restrict the present analysis to low Galactic latitudes, $|b| \leqslant 10°$, where ISM absorption is stronger.

3. Results

Frequency of the $1.5723\,\mu$m DIB: Of the $\sim$60 000 stars included in APOGEE's first year sample, $\sim$12 000 met the selection criteria defined above. From this subsample, we detect the the $1.5723\,\mu$m DIB feature in about 7 000 stars ($\sim$60%). This implies that the corresponding carrier is commonly found in the ISM. The absorption depth of the detected systems range from about 1 to 15% of the continuum level, with typical widths of σ ranging from $1-4$ Å. We find the equivalent width EqW($1.5723\,\mu$m) to span more than an order of magnitude, from about 0.05 to 2 Å.

Correlation with Extinction: In Figure 1a we show the correlation between EqW($1.5723\,\mu$m) and the line-of-sight extinction $A(K_s)$ of the background stars. These extinction values were calculated from individual stellar color excesses, using the RJCE method (Majewski *et al.* 2011). We emphasize that this quantity represents the *foreground* extinction towards each star, rather than the integrated Galactic extinction along the line of sight obtainable from global dust maps (e.g., Schlegel *et al.* 1998, hereafter "SFD"). Thus we expect the RJCE extinction values to reflect the same ISM column density as that harboring the DIB carrier. Indeed, we see a tight correlation between EqW($1.5723\,\mu$m) and extinction, probed over a range equivalent to $\sim$8 mag of $A(V)$. We note that our DIB sample only contains features detected at a significance greater than 2σ, a selection effect that causes the apparent change of slope seen at low column densities.

In Figure 1b, we compare the same EqW($1.5723\,\mu$m) values to the SFD $E(B-V)$ values at the position of each star. As expected, the scatter increases, likely due largely
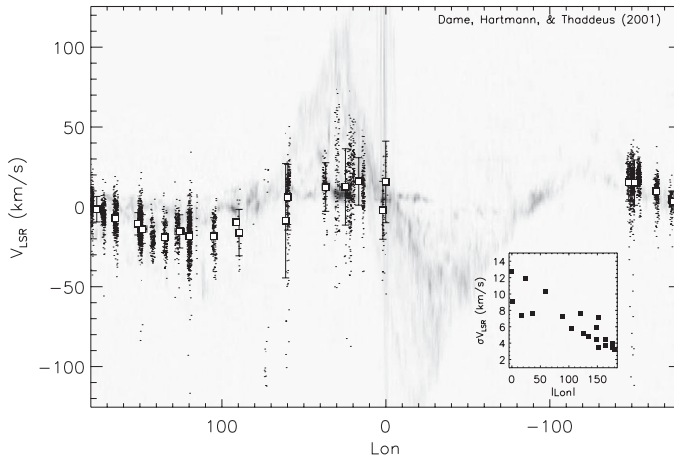
Figure 2. Longitude-velocity plot of integrated $|b| < 10°$ CO emission (greyscale) and the 1.5723 μm DIBs (black and white points). The inset shows the dispersion in DIB velocities as a function of longitude.

to the fact that $E(B-V)$ here, derived from 100 μm emission, probes ISM to the edge of the MW's disk, not just foreground to the star. In addition, the SFD maps have known systematics in regions of high extinction and steep extinction gradients (e.g., SFD; Arce & Goodman 1999; Chen *et al.* 1999), which describes much of the midplane probed by our sample.

Kinematical properties: Given the wide distribution of background sources throughout the Galactic disk, a natural step is to look for *kinematical* correlations with other tracers of the ISM. Because the carrier of the 1.5723 μm DIB is unknown, there is no theoretical basis for determining the feature's intrinsic rest wavelength λ_0; we use the narrow range of fitted Gaussian centers towards the Galactic Center to determine our nominal λ_0 of 1.5723 μm, which is entirely consistent with the published discovery wavelength from Geballe *et al.* (2011).

Assuming our nominal λ_0 is the rest wavelength of the DIB, we measure the velocity of the feature in each $R(\lambda)$, and in Figure 2 we compare them to the velocities of the midplane CO emission (Dame *et al.* 2001), as a function of longitude. The black points are the measurements from the individual stellar spectra, and the white squares indicate the median values in each 10° longitude bin. The sinusoidal longitude-velocity behavior of the Galactic disk is clearly visible in both tracers, and overall, the DIB follows the CO very well. Furthermore, as shown in the Figure 2 inset, the dispersion in DIB velocities at a given longitude decreases towards the outer Galactic disk.

Correlation with other H-Band DIBs: The 1.5723 μm DIB explored thus far is the strongest one known in the *H*-band and the only one consistently measurable in the majority of the APOGEE sample. To extract weaker features, we created median composite spectra and fit single Gaussians to the detected composite absorption profiles. We experimented with various selections and combinations of spectra to include in the composite to maximize the final S/N. For the results shown below, we combined the 25 spectra with the smallest uncertainties in the fitted 1.5723 μm Gaussian center in each 7 deg^2 APOGEE pointing, after shifting each spectrum to the rest wavelength frame of that DIB feature.
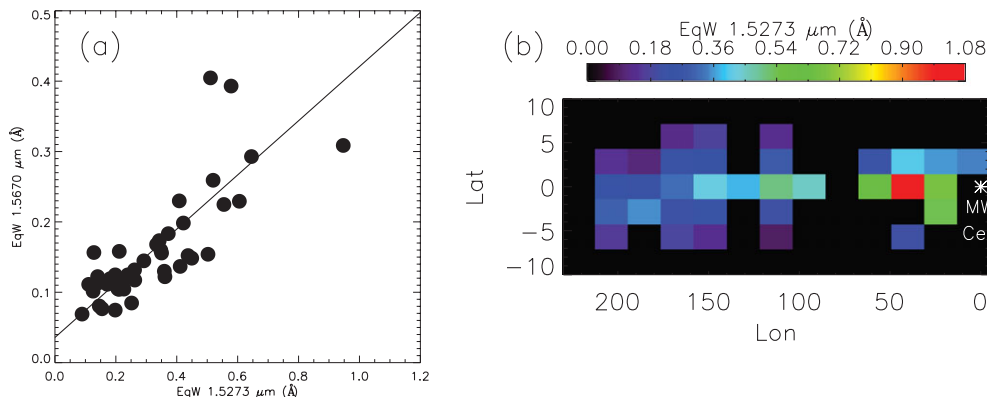
Figure 3. (a): Comparison of equivalent widths of 1.5723 μm and 1.5670 μm DIBs as measured in composite spectra. (b): Distribution of median EqW(1.5723 μm) values in the Galactic midplane.

In Figure 3a, we compare the EqW(1.5723 μm) values from the composite spectra with the values for one of the weaker DIB features, at 1.5670 μm. The strong correlation ($r = 0.86$) suggests similarity and co-existence of the carriers. Such a correlation also implies that we may be able to use the feature centers of well-measured DIBs, like the one at 1.5723 μm, to constrain the rest wavelength (and hence the physical carrier) of weaker DIBs.

Spatial Distribution: As samples of stars with well-measured DIBs have increased in size, some groups have begun mapping their absorption in specific regions, such as star-formation sites (e.g, van Loon *et al.* 2013). We can also construct maps of the DIB EqW, albeit at lower spatial resolution, but over a much larger area. Figure 3b shows the EqW(1.5723 μm) value measured from the median-stacked spectra described above, in $20° \times 3.5°$ pixels, where black indicates regions with no APOGEE data. We note the clear DIB EqW gradients toward the Galactic anti-center at $l = 180°$ and toward higher $|b|$. The notably strong features near $(l, b) \sim (30°, 0°)$ are particularly interesting, as that line of sight intersects a number of star-forming regions and variety of ISM environments, near the junction of the Long Bar and the Norma/Scutum spiral arms.

The large sample of near-IR DIBs presented here probes the Galactic ISM up to several kiloparsecs from the Sun in some of the dustiest regions of the bulge and disk. The sample's size and spatial extent highlight the effectiveness of DIBs as valuable tools in statistical studies of the structure and kinematics of the Milky Way's ISM.

References

Arce, H. G. & Goodman, A. A. 1999, *ApJ* (Letters), 512, L135
Chen, B., Figueras, F., & Torra, J., *et al.* 1999, *A&A*, 352, 459
Dame, T. M., Hartmann, D., & Thaddeus, P. 2001, *ApJ*, 547, 792
Drosback, M. M., Snow, T. P., Thorburn, J. A., *et al.* 2005, IAU Symposium, 235, 256P
Eisenstein, D. J., Weinberg, D. H., Agol, E., *et al.* 2011, *AJ*, 142, 72
Geballe, T. R., Najarro, F., Figer, *et al.* 2011, *Nature*, 479, 200
Heger, M. L. 1922, Lick Observatory Bulletin, 10, 141
Hobbs, L. M., York, D. G., Snow, T. P., *et al.* 2008, *ApJ*, 680, 1256
Hobbs, L. M., York, D. G., Thorburn, J. A., *et al.* 2009, *ApJ*, 705, 32
Joblin, C., D'Hendecourt, L., Leger, A., & Maillard, J. P. 1990, *Nature*, 346, 729
Majewski, S. R., Zasowski, G., & Nidever, D. L. 2011, *ApJ*, 739, 25

Majewski, S. R. 2012, American Astronomical Society Meeting Abstracts #219, 219, #205.06

McCall, B. J., Rachford, B. L., Snow, T. P., *et al.* 2002, NASA Laboratory Astrophysics Workshop, 138

Merrill, P. W. 1936, *ApJ*, 83, 126

Raimond, S., Lallement, R., Vergely, J. L., Babusiaux, C., & Eyer, L. 2012, *A&A*, 544, A136

Schlegel, D. J., Finkbeiner, D. P., & Davis, M. 1998, *ApJ*, 500, 525

van Loon, J. T., Bailey, M., Tatton, B. L., *et al.* 2013, *A&A*, 550, A108